

# Comparisons of direct and adaptative optimal controls for interior permanent magnet synchronous integrated starter generator

L. Chédot\*<sup>†</sup>

<sup>†</sup>Valeo Electrical System  
2, rue A. Boule / BP150  
94017 Créteil Cedex / France  
Email: laurent.chedot@utc.fr

G. Friedrich\*

\*University of Technology of Compiègne  
Electromechanical laboratory / BP20529  
60205 Compiègne Cedex / France  
Email: guy.friedrich@utc.fr

**Abstract**—Integrated Starter Generator (ISG) applications impose very high constraints. So, classic control laws, based on linear models [1] become unadequate. This paper describes two optimal controls (total losses minimisation) based on a numerical, non linear constrained optimisation routine. Optimal computed currents are applied as current references to a machine with various temperatures. This paper shows that Adaptative Optimal Control (AOC) is required to maintain performances of ISG. Without the AOC, efficiencies are reduced but the main problem is a drastic reduction of the maximal mechanical power output in the motor mode.

## I. INTRODUCTION

The study of ISG application leads to make comparisons between different machines structures: induction machine, wound rotor synchronous machine, reluctant and permanent magnet machine ([?], [2]–[5]). All these machines must respect very strong rules and specifications (low size, high torque, speed and efficiency). In this context, IPM structure owns lots of advantages: high specific power, brushless, no losses in the rotor. IPM particularities, associated to ISG constraints (wide speed range, battery supply and highly variable temperature) impose a precise control. After a presentation of the machine design, ISG constraints and control structure, models of the IPM and its environment will be detailed including electromechanical calculations. Then, optimisation procedure will be established. In a final part, two control systems will be compared:

- Direct Optimal Control (DOC)
- Adaptative Optimal Control (AOC)

For a direct optimal control, optimal currents will be computed for a "reference case" and applied to the system (ISG) without taking its evolution into account (for example the temperature).

For an adaptative optimal control, optimal control laws are fitted to the real state of the system. For example, optimal control laws will be computed (off line) for various machine temperatures and will be applied on the machine as a function of its real temperature (measured).

In this paper we compare the performances differences between DOC and AOC for a variable temperature of the machine.

## II. MACHINE AND CONTROL STRUCTURE

### A. Design

Figure 1 shows a cross-section of a classical IPM adapted to flux-weakening operation ([6], [7]).

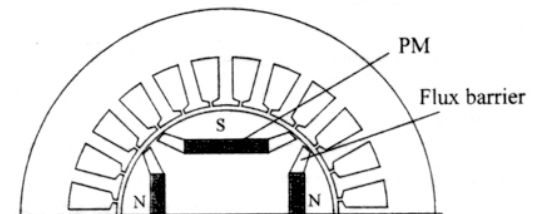


Fig. 1. IPM cross-section [6]

This structure cumulates the characteristics of permanent-magnet and reluctant machines [8]: torque is a combination of hybrid and reluctant torque; the induced voltage, due to the presence of permanent-magnet excitation, is constant and must be reduced by flux-weakening at high speed. Electrical and mechanical behaviour will be detailed in section III.

### B. Constraints due to starter-generator application

Starter-generator, as others automotive applications, is very constrained:

- low size;
- high torque at low speed with minimum power taken on the battery (140 Nm at 600  $A_{rms}$ , 8 kW);
- operating points at high speed ( $\rightarrow$  6000 rpm);
- power and voltage limited by battery: 8kW, 21 to 36 V in Motor mode (starter or boost) and 42 to 50V in Generator mode (power depending on battery technology);
- limited battery energy storage;
- current limited by inverter or thermic conditions (150  $\rightarrow$  600  $A_{rms}$ );
- high temperature variation (25°C  $\rightarrow$  180°C).

These constraints create specific behaviours (high magnetic saturation) and limitations (current, voltage, power, energy).

Moreover, terminal voltage, equal to the battery voltage, varies with the state of charge and the consumed power.

### C. Control scheme

This machine is used as starter and generator. Its control is unified by using unique torque control; positive torques for motor operations, and negative for generator. Figure 2 shows this control scheme.

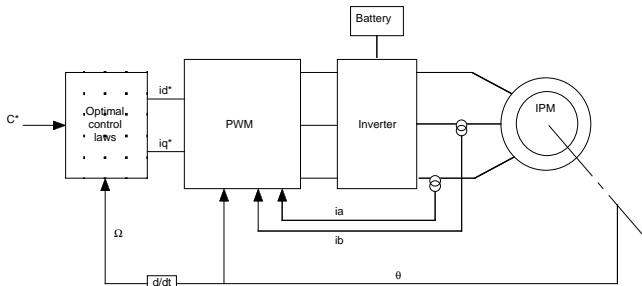


Fig. 2. Optimal torque control

The optimal control laws, including flux-weakening [9], [10], can be explained thanks to the circle diagram and the three control modes introduced by MORIMOTO and all. in [1]. In order to use simple analytical expression, a lot of hypotheses must be done: no magnetic saturation, constant terminal voltage, no temperature variation.

*We show that, in the starter-generator application, these hypotheses can not be maintained. In these conditions, to realise a precise control including high efficiency, it becomes necessary to take into account all the non-linearities (machine and application) in a specific control.*

One way is to compute, by numerical calculations, MORIMOTO's ideal trajectories with precise models of the machine.

## III. MODELS

### A. Machine

The IPM is modelised by classical Park's equations [11] (d-q reference frame) except for flux and iron power losses.

1) *Saturation*: Because of magnetic saturation, flux can not be expressed as functions of inductances. Each flux  $\psi_{dq}$  is a non-linear function of the currents  $i_{dq}$ .

$$\psi_d = f_d(i_d, i_q) \quad (1)$$

$$\psi_q = f_q(i_d, i_q) \quad (2)$$

$f_{dq}$  are calculated by interpolation of measures tables realised with the finite element (FE) software FLUX2D [12]. For different operating points ( $i_{dq}$ ), and in presence of the permanent magnets, the 3 phase flux ( $\psi_{abc}$ ) are evaluated (internal function) and so, direct and quadrature flux are deduced.

2) *Iron losses*: Iron losses evaluation follow the same procedure, FE measurements (FLUX2D) for different speed and different operating points give tables of data which are interpolated. After the prototype construction, iron losses will be measured and the characteristics will be used for the optimisation.

$$P_{iron} = f(i_d, i_q, \omega_s) \quad (3)$$

### B. Inverter

Inverter behaviour is considered as ideal. Its global efficiency and load voltage drops on the power switches can be added easily.

### C. Battery

Battery is modelled by a voltage source in series with an internal resistance as shown on figure 3.

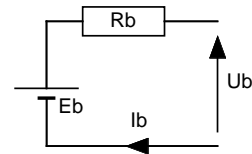


Fig. 3. Battery electrical model

Maximum power supply is equal to:

$$P_{bmax} = \frac{E_b^2}{4R_b} \quad (4)$$

In generator mode, terminal voltage is regulated at a constant value (around). Battery is so modelled by a simple voltage source  $V_{ch}$ .

### D. Electromechanical equations

For a given operating point ( $i_d$ ,  $i_q$  and  $\omega_s$ ), all electrical and mechanical data are performed:

- current (RMS),

$$I_{rms} = \sqrt{\frac{i_d^2 + i_q^2}{3}} \quad (5)$$

- flux (table),

$$\psi_{dq} = \psi_{dq}(i_d, i_q) \quad (6)$$

- iron (table) and total losses,

$$P_{iron} = P_{iron}(i_d, i_q, \omega_s) \quad (7)$$

$$P_{losses} = P_{iron} + 3R_s I_{rms}^2 \quad (8)$$

- electromagnetic, losses and mechanical torque,

$$T_{em} = p[\psi_d i_q - \psi_q i_d] \quad (9)$$

$$T_{iron} = \frac{P_{iron}}{\Omega} \quad (10)$$

$$T_m = T_{em} - T_{iron} \quad (11)$$

- voltage,

$$v_d = R_s i_d - \omega_s \psi_q \quad (12)$$

$$v_q = R_s i_q + \omega_s \psi_d \quad (13)$$

$$V_{rms} = \sqrt{\frac{v_d^2 + v_q^2}{3}} \quad (14)$$

- electrical and mechanical power,

$$P_e = v_d i_d + v_q i_q \quad (15)$$

$$P_m = T_m \Omega \quad (16)$$

- efficiency,

$$\eta = \left( \frac{P_m}{P_e} \right)^{\text{sign}(T_m)} \quad (17)$$

- battery voltage,

$$U_b = \frac{E_b + \sqrt{E_b^2 - 4R_b P_b}}{2} \quad (18)$$

where  $P_b$  is the power given by the battery. It is equal to the electrical power divided by the inverter efficiency. If voltage are considered as sinusoidal, across voltage supply is equal to:

$$V_{sup} = \frac{U_b}{2\sqrt{2}} \quad (19)$$

- The maximum injectable current is equal to the maximum inverter current in starter mode and is limited by the maximum current density in the IPM in generator mode:

$$I_{lim} = \begin{cases} I_{inverter\ max} & (starter) \\ \propto J_s\ max & (generator) \end{cases} \quad (20)$$

#### IV. OPTIMISATION PROCEDURE

##### A. Principle

Controlling the IPM is equivalent to injecting the currents  $i_{dq}$  which minimise the total losses with respect to different constraints (torque, current, voltage and power).

$$\forall (T^*, \Omega), \quad (i_d^*, i_q^*) \setminus \min_{i_d^*, i_q^*} \sum P_{losses}$$

with

$$\begin{aligned} T_m &= T^* \\ V_{rms} &\leq V_{disp} \\ I_{rms} &\leq I_{lim} \\ P_e &\leq P_{bmax} \end{aligned}$$

The MATLAB optimisation toolbox [13] provides a non-linear constrained optimisation routine. It minimises an *objective function*  $f$  and tries to maintain *constrained functions*  $g$  negative:

$$x^* \setminus \min_{x^*} f(x^*)$$

with

$$g_i(x^*) < 0, \quad \forall i = 1..N_{constraints}$$

##### B. Objective function

The objective function is here the total losses (Cf. equation 7):

$$f = P_{losses} \quad (21)$$

##### C. Constraints function

The constraints functions are:

- Mechanical torque (Cf. equation 11) is equal to the order torque:

$$g_t = |T_m - T^*| - \epsilon |T^*| \quad (22)$$

$\epsilon$  is a percentage ( $0 < \epsilon < 1$ ) which defines precision.

- Current (Cf. equation 5) is less than the limit (Cf. equation 20):

$$g_i = I_{rms} - I_{lim} \quad (23)$$

- across voltage (Cf. equation 14) is less than the available voltage (Cf. equation 19)

$$g_v = V_{rms} - V_{sup} \quad (24)$$

- In starter mode, electrical power (Cf. equation 15) is limited by the battery maximum power (Cf. equation 4):

$$g_p = P_e - P_{bmax} \quad (25)$$

##### D. Algorithm

- 1) The operating range is established. Speed is due to the application: from 0 to the application maximum speed (5000 rpm). Maximum and minimum torques are calculated at standstill by a first constrained optimisation.
- 2) For each couple  $(T^*, \Omega)$ ,  $i_{dq}^*$  are calculated by optimisation as seen before.

#### V. APPLICATION

As an application, two optimal control will be compared:

- Direct Optimal Control (DOC)
- Adaptative Optimal Control (AOC)

For a direct optimal control, optimal currents will be computed for a "reference case" and applied to the system (ISG) without taking its evolution into account (for example the temperature).

For an adaptative optimal control, optimal control laws are fitted to the real state of the system. For example, optimal control laws will be computed (off line) for various machine temperatures and will be applied on the machine as a function of its real temperature (measured).

In this section we compare the performances differences between DOC and AOC for a variable temperature of the machine.

##### A. Direct optimal control

Reference conditions: temperature is close to the ambient temperature ( $T = 25^\circ C$ ), stator resistance is therefore equal to:  $R_s = 6.1\ m\Omega$ . In starter mode, current is limited by inverter:  $I_{lim} = 600\ A_{rms}$ ; and voltage by battery:  $E_b = 36\ V$ ,  $R_b = 40\ m\Omega$ . In generator mode, current is limited by current density in IPM:  $J_s \leq 10\ A/mm^2 \Rightarrow I_{lim} < 190\ A_{rms}$ ; and voltage by the regulation:  $V_{sup} = \frac{V_{ch}}{2\sqrt{2}}$ ,  $V_{ch} = 42\ V$ .

Optimal laws are computed for the reference case. These laws are applied to the IPM in reference conditions.

1) *Performances for DOC and reference temperature conditions:* We can see on figure 4 efficiencies in the torque vs. speed plan.

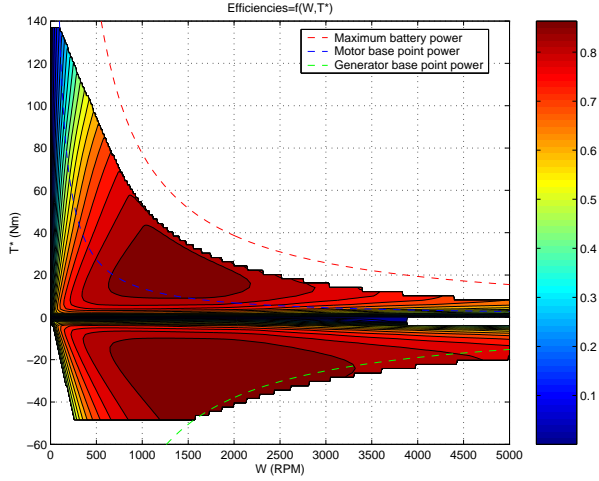


Fig. 4. Efficiencies in torque vs. speed plan

Positive torques represent the starter mode, and so negative torques, the generator mode. We can see lots of differences between these two kinds of operating modes:

- maximum torque is limited by the highest injectable current and the maximum electrical power. In generator, thermic conditions in steady-state limit current density;
- base speed and covered area are directly affected by the voltage limitation. Even with our simple model of battery, the influence of the terminal voltage decreasing is very important in terms of operating range;
- in generator mode, some operating points are not accessible. For low torque or low speed, the mechanical power is not sufficient to compensate the losses (copper and iron).

2) *Performances for DOC and high temperature conditions:* Starter-generator machine is located in the thermal engine block. Temperature should rise quickly in standard drive conditions. Stator winding temperature is so estimated at  $180^{\circ}C$ . At this temperature, stator resistance rises from  $6.1\ m\Omega$  to  $9.9\ m\Omega$ .

Figure 5 presents the difference of efficiencies in the case where optimal laws are applied to the IPM in the reference conditions and in the high temperature conditions.

With a current control, stator resistance variation has only an effect on voltage and copper losses. As a consequence:

- Generator operating limit, due to the maximum current density, is not affected.
- Starter operating limit is reduced. For a given current, phase voltage and electrical power are increased. Voltage limit is reduced whereas IPM needs more voltage. Voltage constraint becomes stronger and the operating

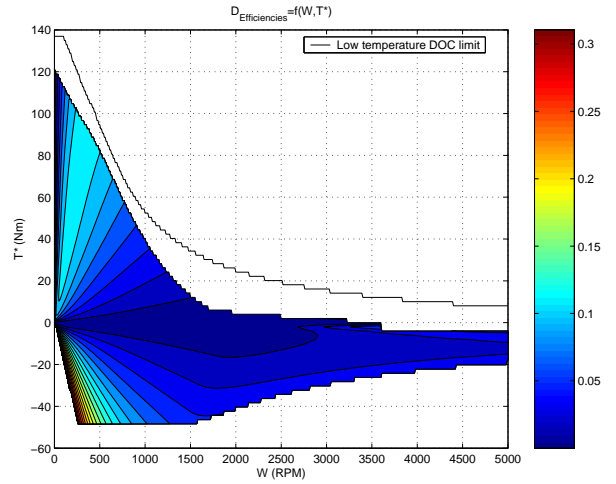


Fig. 5. Efficiencies variations in torque vs. speed plan for DOC and high temperature conditions

limit decreases. For example: at  $2000\ rpm$ , the IPM in the reference conditions can develop more than  $5\ kW$  of mechanical power. At the same speed, when optimal laws are applied to the IPM in high temperature conditions, any mechanical power can be delivered.

- In the whole operating range, efficiencies are decreased because of copper losses increase. The difference is everywhere about the same. For example, at  $2000\ rpm$  in generator mode, the IPM in reference conditions and controlled by the optimal laws delivers its maximal power with an efficiency of 0.85. With the same operating points, the machine in high temperature conditions has an efficiency of only 0.8.

3) *Performances for AOC and high temperature conditions:*

In reference conditions, performances are of course the same as in figure 4. In contrast, figure 6 shows the performances obtained in an AOC (to be compared with the figure 5 for operating range and figure 4 for efficiencies).

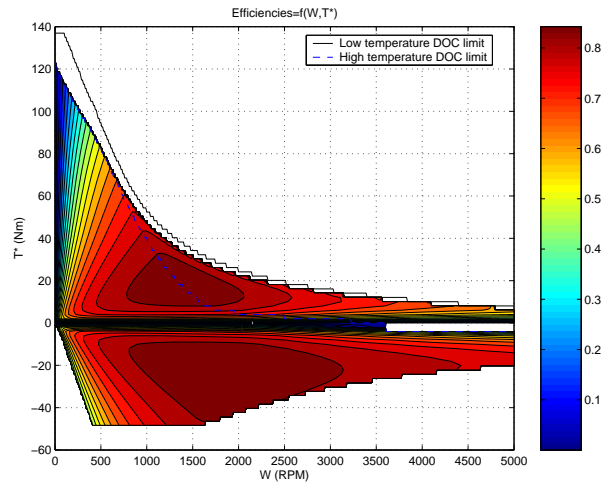


Fig. 6. Efficiencies in torque vs. speed plan for AOC and high temperature conditions

By comparing DOC and AOC at high temperature conditions, we can see:

- at low speed, limits and efficiencies are equal;
- when speed is increasing, operating points, not accessible in DOC, became realisable in AOC, and moreover, mechanical power and efficiencies are always high.

When adaptive laws are used, IPM performances are always at the maximal possibilities. Flux-weakening is available in high speed, and efficiencies remain high.

Table I shows the comparaison between maximal mechanical power and efficiency at 2000 rpm (previous example).

TABLE I  
MAXIMAL MECHANICAL POWER AND EFFICIENCY AT 2000 rpm  
(EXAMPLE)

Control and conditions	DOC (low temperature)	DOC (high temperature)	AOC (high temperature)
Maximal mechanical power	5 kW	800 W	4 kW
Efficiency	0.8	0.7	0.8

## VI. CONCLUSION

This paper has examined the principle of two optimal control of interior permanent magnet synchronous machine in the starter-generator application. It has been shown that IPM particularities (permanent magnet, reluctant torque) require a precise control. The strong constraints of the ISG application, particularly the magnetic saturation and the voltage supply, have highlighted the necessity of taking into account all these non-linearities in an optimal control. This control was established by classical optimal calculation. We have shown that AOC is required to maintain performances of ISG. Without the AOC, efficiencies are reduced but the main problem is a drastic reduction of the maximal mechanical power output in the motor mode.

## REFERENCES

- [1] S. MORIMOTO, Y. TAKEDA, T. HIRASA, and K. TANIGUCHI, "Expansion of operating limits for permanent magnet motor by current vector control considering inverter capacity," *IEEE Trans. Ind. Appl.*, vol. 26, pp. 866–871, Sep./Oct. 1990.
- [2] B. CHALMERS, L. MUSABA, and D. GOSDEN, "Variable-frequency synchronous motor drives for electrical vehicles," *IEEE Trans. Ind. Appl.*, vol. 32, no. 4, pp. 896–903, Jul./Aug. 1996.
- [3] E. LOVELACE, T. JAHNS, J. KIRTLEY, and J. LANG, "An interior PM starter-alternator for automotive applications," in *Int. Conf. Electrical machines*, Istanbul, Sep. 1998, pp. 1802–1808.
- [4] J. HADJI-MINAGLOU and G. HENNEBERGER, "Comparison of different motor types for electric vehicle application," *EPE Journal*, vol. 8, no. 3-4, pp. 46–55, Sep. 1999.
- [5] G. FRIEDRICH, L. CHÉDOT, and J. BIEDINGER, "Comparison of two optimal machine design for integrated starter-generator applications," in *Int. Conf. Electrical machines*, Aug. 2002.
- [6] N. BIANCHI, S. BOLOGNANI, and M. ZIGLIOTTO, "High-performance PM synchronous motor drive for an electrical scooter," *IEEE Trans. Ind. Appl.*, vol. 37, no. 5, pp. 1348–1355, Sep./Oct. 2001.
- [7] C. HWANG and Y. CHO, "Effects of leakage flux on magnetic fields of interior permanent magnet synchronous motors," *IEEE Trans. Mag.*, vol. 37, no. 4, pp. 3021–3024, Jul. 2001.
- [8] T. MILLER, *Brushless Permanent Magnet and Reluctant motor drive*. Oxford university press, 1989.

- [9] W. SOONG and T. MILLER, "Field-weakening performance of brushless synchronous AC motor drives," *IEE Proc. - Elec. Power Appl.*, vol. 141, no. 6, pp. 331–340, 1994.
- [10] B. MULTON, J. LUCIDARNE, and L. PRÉVOND, "Analyse des possibilités de fonctionnement en régime de désexcitation des moteurs à aimants permanents," *Journal Physique III*, pp. 623–640, 1995.
- [11] G. SÉGUIER and F. NOTELET, *Electrotechnique industrielle*. Technique et documentation, 1994.
- [12] *Analyse des dispositifs électriques, magnétiques et thermiques par la méthode des éléments finis. Notice d'utilisation générale*, Cedrat, Oct. 1996.
- [13] *Optimization toolbox user's guide for use with Matlab*, The MathWorks Inc., 2000.